Available online at www.sciencedirect.com
SCIENCE DIRECT®
Journal of Chromatography A, 1078 (2005) 162–170
JOURNAL OF CHROMATOGRAPHY A
www.elsevier.com/locate/chroma

# Efficiency for unretained solutes in packed column supercritical fluid chromatography II. Experimental results for elution of methane using large pressure drops

Wensheng Xu [1], Dawn L. Peterson [2], Jonathan J. Schroden [3], Donald P. Poe *

*Department of Chemistry, University of Minnesota Duluth, 10 University Drive, Duluth, MN 55812, USA*

Received 14 January 2004; received in revised form 2 August 2004; accepted 4 May 2005

**Abstract**

At near-critical temperatures and pressures, experimental results for elution of methane with neat carbon dioxide on a 150 mm × 2.0 mm I.D. column packed with 5 μm porous silica with a bonded octylsilica stationary phase show much greater efficiency losses than predicted by theory if isothermal conditions are assumed. Experiments with insulated, air- and water-thermostatted columns demonstrate that significant axial and radial temperature gradients are produced by Joule–Thomson cooling of the mobile phase, and that radial temperature gradients can be a major cause of band spreading at low temperatures and pressures. The use of thermal insulation on the column can greatly improve efficiency under these conditions.


*Keywords:* Supercritical fluid chromatography; Efficiency; Pressure drop; Temperature drop

## 1. Introduction

This is the second of two papers in which we address some unresolved questions about efficiency losses associated with large pressure drops in packed-column supercritical fluid chromatography (pSFC). The first paper [1] presented the theory and a model for elution of unretained solutes under isothermal conditions, and concluded that efficiency losses should not exceed 20% even under extreme conditions. Other theoretical treatments cited in that paper also assume isothermal conditions either explicitly or implicitly. There are at least a few reports, however, that deal with the development of temperature gradients at large pressure drops due to expansion of the mobile phase in the column. Schoenmakers et al. [2] calculated pressure, density and temperature profiles in pSFC with modest pressure drops and concluded that temperature gradients are not a major source of concern. In other reports, significant temperature drops were observed when using low column outlet pressures (<100 bar) and pressure drops up to 20 bar [3,4]. These latter reports suggest that the assumption of isothermal conditions when large pressure drops are used may not be valid.

In this study we compare the experimental results obtained for elution of methane under large pressure drops and different thermal conditions to the predicted behavior for isothermal conditions. Based on these observations, we evaluate the relative contributions of mobile phase expansion and temperature gradients to efficiency loss, and make recommendations for avoiding excessive efficiency loss under these conditions.

* Corresponding author. Tel.: +1 218 726 7212; fax: +1 218 726 7394.
*E-mail address:* dpoe@d.umn.edu (D.P. Poe).
[1] Present address: P&G Pharmaceuticals, Norwich, NY 13815, USA.
[2] Present address: Department of Chemistry, College of Saint Scholastica, Duluth, MN 55812, USA.
[3] Present address: The CNA Corporation, Alexandria, VA 22311-1850, USA.

0021-9673/$ – see front matter © 2005 Elsevier B.V. All rights reserved.
doi:10.1016/j.chroma.2005.05.001

## 2. Experimental

### 2.1. Apparatus

The SFC system was constructed in our laboratory and was described earlier in detail [3]. Briefly, it consisted of an ISCO model 260D syringe pump, a helium-actuated Valco CI4W injector with a 60 nL or 500 nL internal sample loop, and a Varian model 2740 gas chromatograph with flame ionization detection (FID) system. The injector was placed in the column oven and a thermal conditioning coil was placed within the oven upstream from the injector to preheat the mobile phase to the column oven temperature. Pressure transducers were connected to tees placed before the injector and at the column outlet, and the column outlet pressure was adjusted with nitrogen. A 40 cm × 30 μm I.D. fused silica restrictor connected the column outlet tee to the FID system, and a secondary restrictor, a heated length of small-bore stainless steel tubing, was provided to accommodate mobile phase flows exceeding the capacity of the primary restrictor.

In early experiments, including all of those using a water-jacketed column, data were acquired using the most sensitive detector setting in conjunction with a strip chart recorder that was actuated with a contact switch at injection. This setup, which resulted in significant peak distortion due to slow response of the detection system, will be referred to as the analog system. In later experiments data were acquired using a computerized data system and a less sensitive detector setting, which yielded a much shorter system time constant and peaks with minimal distortion. This configuration will be referred to as the digital system. Results from experiments using both configurations are included in this paper.

The column was 150 mm × 2.0 mm I.D. stainless steel packed with 5 μm Spherisorb C8 (Waters, Milford, MA, USA). The same column (A) was used for all of the experiments using the analog system. A second identical column (B) from Waters was used with the digital system. For studies on the effects of thermal conditions, the column was configured in one of three ways. For the uninsulated (air-thermostatted) case, the steel walls of the column were exposed to the oven air in typical fashion. For the insulated case, the column was covered with fiberglass and foam pipe insulation as described earlier [4]. For the water-thermostatted case, the column was enclosed within a water jacket fashioned from PVC pipe and fittings, and water thermostatted at the column oven temperature ±0.1 °C was circulated through the jacket.

The column inlet and outlet temperatures were monitored with small button-style surface-probe thermocouples. The probes were attached to the nuts which secure the connector tubing pieces to the column end fittings by wrapping the probe and nut with adhesive tape so that the probe was in direct contact with the connector nut. Several wrappings of tape provided a modest amount of insulation of the probe and nut from the column oven. For the insulated case, the column insulation was extended over the ends to include the thermocouple probes and connector nuts. The temperature-measuring units were calibrated against a third calibrated mercury thermometer. The accuracy, readability and repeatability of the temperature measurements were ±0.1 °C.

### 2.2. Chemicals

Carbon dioxide was SFC grade with no helium. Methane was 99 mol% pure. Both were obtained from Scott Specialty Gases, Troy, MI, USA. Solutions of methane in $CO_2$ were prepared by introducing gaseous methane at ambient pressure into an open 150 $cm^3$ stainless steel vessel, displacing most of the air. The vessel was then sealed with a threaded plug on one end, and liquid $CO_2$ was introduced through a valve with an integral pressure relief port on the opposite end to a pressure of 80 bar at ambient temperature. The vessel was then sealed by closing the valve and disconnected from the $CO_2$ supply, and a connection was made between the valve and the sample port of the injector with a length of 1/16 in. O.D. stainless steel tubing as described earlier [3]. Loading sample into the injector was accomplished by temporarily opening a valve connected to the waste port and allowing the pressurized sample to vent through a restrictor fabricated from a short length of 1/16 in. O.D. stainless steel tubing which was crimped on the end.

### 2.3. Chromatography

Methane in $CO_2$ was introduced into the injector from the pressurized vessel as described above. Isopycnic (constant density) plate height curves were generated by adjusting the inlet and outlet pressures independently to achieve the desired flow rate so that the temporal average mobile phase density remained constant for all combinations of inlet and outlet pressure, assuming isothermal conditions. The mobile phase in the syringe pump was maintained at −2.0 °C, and the detector temperature was 250 °C. Injections for each set of conditions were done in triplicate, and an equilibration time of 10–15 min was allowed after changes in the inlet and outlet pressures. A constant flow rate at the pump and a constant temperature at the column outlet were taken to indicate steady-state flow and thermal conditions.

### 2.4. Data treatment

As noted above, chromatographic data were obtained using either a strip chart recorder (analog system) or a computerized data system (digital system). In either case the basic approach to calculating fundamental chromatographic variables was the same, except in terms of accounting for extra-column band spreading. No attempt was made to correct for extra-column sources of band spreading and peak distortion in the analog data. For experiments with the digital system, extra-column contributions to band spreading were measured and corrections were applied.

The peak width at half height $w_h$ for three successive chromatograms was measured and the apparent plate height was calculated as

$$\hat{H} = L\frac{w_h^2}{5.545t_r^2} \quad (1)$$

and the reduced velocity was calculated as

$$\nu = \frac{Ld_p}{t_r D_m} \quad (2)$$

where $t_r$ is the retention time, $L$ is the column length, $d_p$ is the particle size, and $D_m$ is the diffusion coefficient of methane in carbon dioxide. The diffusion coefficient was evaluated at the temporal average density of the mobile phase using the equation of Wilke and Chang as modified by Sassiat et al. [5] for supercritical $CO_2$.

## 3. Results and discussion

### 3.1. Principal equations

The theoretical treatment given in the previous paper [1] concluded that under isothermal conditions the apparent plate height for an unretained solute is adequately represented by the approximate relation

$$\hat{h} \cong f_1 h \quad (3)$$

where $f_1$ is the compressibility correction factor and $h$ is the local plate height. The correction factor is given by

$$f_1 = \frac{\langle\rho\rangle_t}{\langle\rho\rangle_z} \quad (4)$$

where $\rho$ is the local mobile phase density, and the brackets with subscripts t and z represent the temporal and spatial averages of the enclosed quantities, respectively. The local reduced plate height, which is determined experimentally at a high mobile phase density, can be expressed by a simplified form of the Knox equation

$$h = \frac{B}{\nu} + A\nu^{1/3} + C\nu \quad (5)$$

where the Knox constants $A$, $B$, and $C$ are independent of the mobile phase conditions, and $\nu$ is the reduced velocity, which is approximately constant under conditions of constant mass flow rate and temperature.

### 3.2. Model calculations for elution of methane

The model described in the previous paper [1] was used to generate predicted plate height curves and the corresponding values of $f_1$ for elution of methane on a column packed with microporous spherical silica particles using neat carbon dioxide as the mobile phase under the experimental conditions used in this investigation. The local retention factor for methane was set equal to zero under all conditions. The model employs reduced densities, $\rho_R = \rho/\rho_c$ where $\rho_c = 0.468$ g/cm$^3$ is the critical density of carbon dioxide. Isothermal conditions are assumed. Isopycnic plate height curves, in which the temporal average mobile phase density remains constant over the entire range of flow rates, are generated in order to facilitate comparison of the data under different conditions.

The inlet and outlet pressures required for all of the predicted and experimental isopycnic plate height curves reported in this study are shown in Fig. 1. The corresponding values of $f_1$ are shown in Figs. 2 and 3. As long as the temporal average reduced density is greater than 1.5, the data for $f_1$ show that the predicted efficiency loss for pressure drops up to 50 bar should be less than 1% (i.e., $f_1 < 1.01$). Taking 1% as an acceptable level of efficiency loss, a column operated at $\langle\rho_R\rangle_t \geq 1.5$ can be regarded as a uniform column, and the experimentally observed plate height measured at the outlet

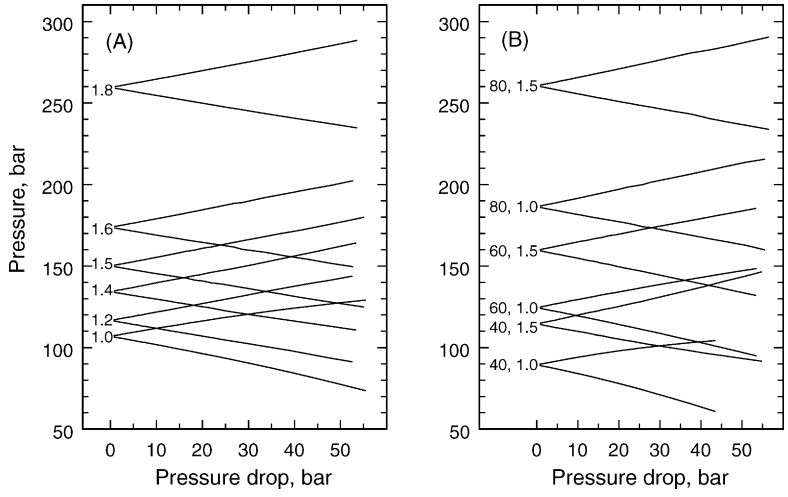


Fig. 1. Inlet and outlet pressures required to achieve constant temporal average density at (A) 50 °C, and (B) 40–80 °C. The temporal average reduced density, and for B the temperature, is given at the left of each pair of curves.

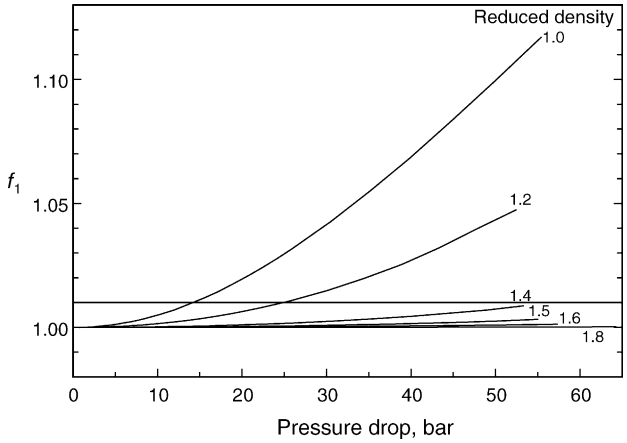


Fig. 2. Effect of pressure drop on $f_1$ for carbon dioxide at 50 °C at different reduced densities. Reference lines are shown for $f_1 = 1.00$ and 1.01.

of the column can be taken as a measure of the local plate height $h$.

Fig. 4 shows a set of predicted isopycnic plate height curves generated by the model for elution of methane on a well-packed column at 50 °C and different densities. The column pressure drop for each curve is also shown on the axis at the right. The curves show a small but significant increase in apparent plate height with decreasing temporal average density at high velocities, consistent with the trends in $f_1$.

### 3.3. Experimental results for methane

The experimental plate height curves obtained for methane at 50 °C and reduced densities 1.0–1.8 using the analog system and column A are shown in Fig. 5. The curves show significant losses of efficiency at lower densities, a trend that is consistent with theoretical predictions, but the losses are much greater than predicted. Our model [1] predicts that for most conditions the increase in apparent plate height should

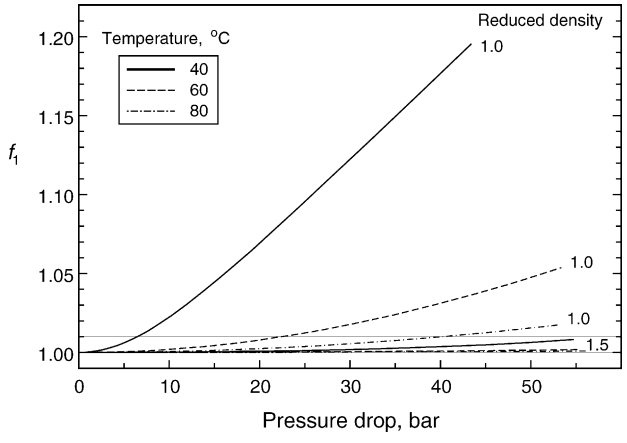


Fig. 3. Effect of pressure drop on $f_1$ for carbon dioxide at 40–80 °C and reduced densities 1.0 and 1.5. Reference lines are shown for $f_1 = 1.00$ and 1.01.

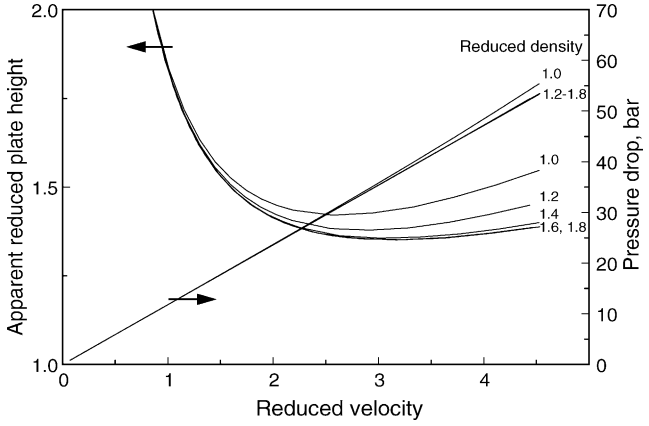


Fig. 4. Predicted plate height curves for elution of methane as an unretained solute with carbon dioxide at 50 °C and various temporal average reduced densities. Parameters for Knox equation: $B = 1.2$, $A = 0.6$, $C = 0.0286$; interparticle porosity = 0.4. See Fig. 1 for inlet and outlet pressures at indicated pressure drops.

be no more than a few percent, and even under the most extreme conditions should not exceed 20%. Although the observed efficiency under all conditions is rather poor due in part to the slow response of the analog data system, this effect should have roughly the same impact on each curve, and we can attribute the relative magnitudes of the plate height to mobile phase effects.

In order to validate these observations, the plate height studies were repeated at reduced densities 1.0 and 1.5 using the digital system and column B. The results are shown in Fig. 6. The data at $\langle \rho_R \rangle_t = 1.5$ are consistent with a well-packed column with no indications of excessive band broadening. At the lower density we again see very large increases in apparent plate height at the higher reduced velocities and pressure drops. Taking the curve at $\langle \rho_R \rangle_t = 1.5$ to represent the uniform column case, we applied Eq. (3) to calculate the predicted plate height at $\langle \rho_R \rangle_t = 1.0$. The predicted curve, shown

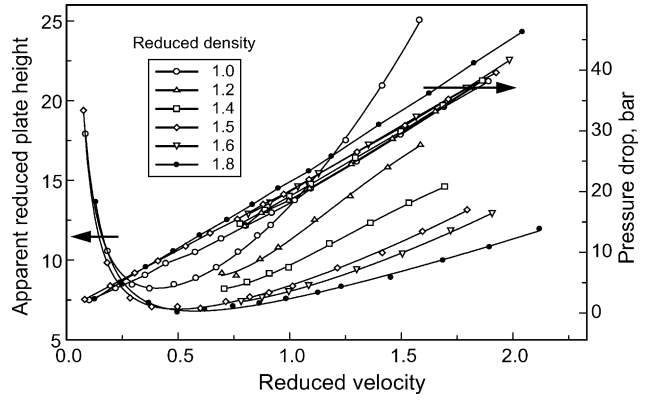


Fig. 5. Experimental isopycnic plate height curves for elution of methane with carbon dioxide at 50 °C and different reduced densities on a 2.0 mm × 150 mm I.D. column packed with 5 μm Spherisorb C8 (column A) with analog data collection. Apparent plate height and pressure drop curves at the same reduced density use the same symbol. See Fig. 1 for inlet and outlet pressures at indicated pressure drops.

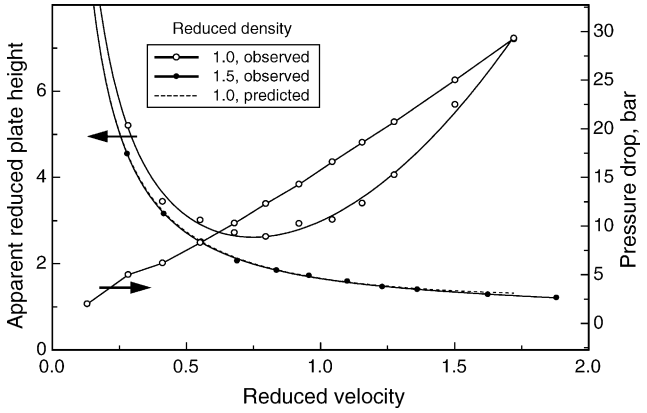


Fig. 6. Experimental and predicted isopycnic plate height curves for elution of methane at 50 °C and reduced densities 1.0 and 1.5 on a 2.0 mm × 150 mm I.D. column packed with 5 μm Spherisorb C8 (column B) with digital data collection. Data are corrected for extracolumn effects. Dashed line is the predicted plate height at $\langle\rho_R\rangle_t = 1.0$ based on observed efficiency at $\langle\rho_R\rangle_t = 1.5$ as the uniform column case. See Fig. 1 for inlet and outlet pressures at indicated pressure drops.

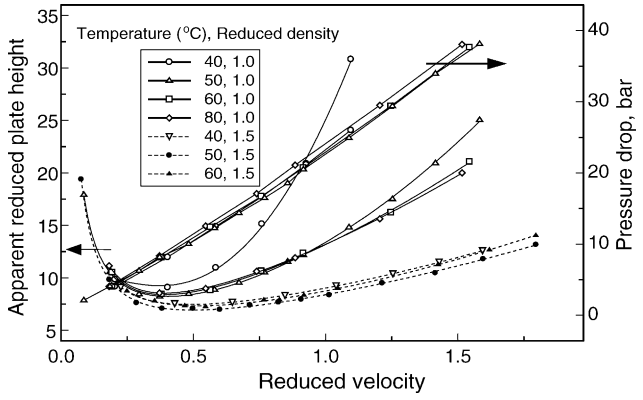


Fig. 7. Experimental isopycnic plate height curves for elution of methane at various temperatures and two reduced densities using column A. See Fig. 5 for other conditions.

as a dashed line in Fig. 6, is nearly indistinguishable from the experimental curve at $\langle\rho_R\rangle_t = 1.5$. However, at $\langle\rho_R\rangle_t = 1.0$ the observed loss in efficiency is clearly much greater than predicted by theory.

The effect of temperature on efficiency loss is shown in Fig. 7. Since the data were obtained using the analog system and column A, we will again focus only on the relative magnitudes of the curves. The curves at $\langle\rho_R\rangle_t = 1.5$ essentially overlap and may be taken to represent the uniform column case. The curves at $\langle\rho_R\rangle_t = 1.0$, however, show an increasing loss of efficiency with decreasing temperature, a trend that is consistent with the data for $f_1$ shown in Fig. 3, but the magnitude of the increase in apparent plate height is again much greater than the maximum predicted increase of about 6% based on the computed values of $f_1$.

We conclude from the foregoing discussion that our model for apparent plate height [1] does not fully explain the observed efficiency losses. We note that the model assumes isothermal conditions. In the following discussion we show that isothermal conditions were not achieved in our experiments, and that the generation of radial temperature gradients in the column is the principal cause of excessive efficiency loss at large pressure drops.

### 3.4. Evidence of a temperature drop in the column

For the plate height studies presented in Figs. 5 and 7, the temperature at the column outlet was monitored as described in Section 2. Because we used a surface probe attached to the connector nut and did not directly probe the mobile phase,

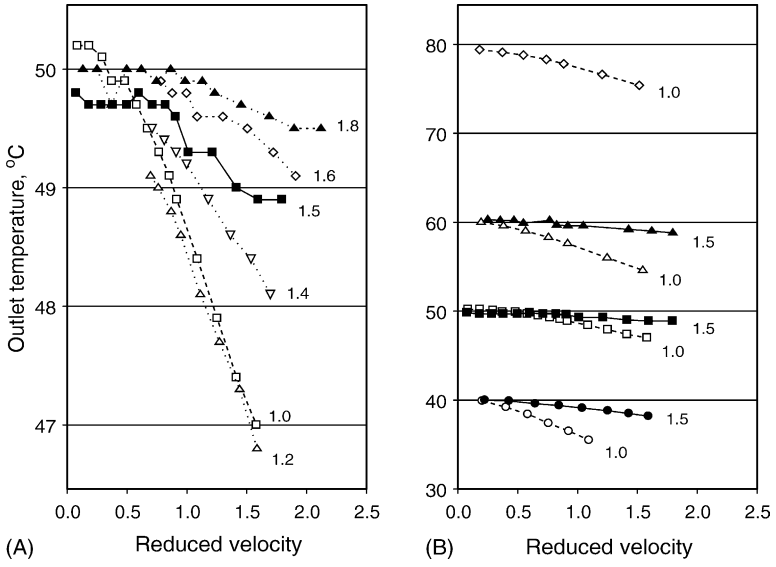


Fig. 8. Column outlet temperature as a function of reduced velocity at various oven temperatures and mobile phase densities. Oven temperatures are (A) 50.0 °C; (B) 40.0, 50.0, 60.0, and 80.0 °C. See Figs. 5 and 7 for operating conditions.

the recorded temperature should be taken only as an approximation of the temperature of the mobile phase at that point.

Plots of column outlet temperature versus reduced velocity are shown in Fig. 8. The inlet temperature was not monitored and is taken to be equal to the oven temperature. In all cases the outlet temperature decreases with increasing reduced velocity, with the largest decreases occurring at the lowest densities. For an oven temperature of 50 °C, temperature drops of up to 3 °C are observed at the lower densities. Even at the highest reduced density of 1.8 (average column pressure = 260 bar) the temperature drop reaches 0.5 °C. Significant temperature drops are seen at both densities for all temperatures studied.

The temperature drop must be a result of the Joule–Thomson effect, and the trends in the temperature data are consistent with the increased compressibility of a fluid near its critical density. The magnitude of the temperature drop, however, is much greater than has generally been recognized [2]. The existence of temperature gradients in HPLC has been identified as a source of band spreading [6,7], where frictional heating at high velocities can generate a positive axial temperature gradient along the column. If the column wall is maintained at constant temperature, this axial gradient will generate a radial temperature gradient with the fluid at the center of the column being warmer than that near the wall. This leads in turn to radial gradients in viscosity and mobile phase velocity, resulting in a parabolic band profile with the leading edge of the band at the center of the column. The net result is an extended solute band, and the phenomenon may be referred to as gradient-induced band spreading [8].

In pSFC we have both frictional heating and Joule–Thomson cooling, and the relative magnitudes of these will result in a net increase or decrease in temperature along the column axis, depending on the operating conditions [2]. Under our experimental conditions we have a net decrease in temperature. By analogy to HPLC, this would lead to a parabolic band profile with the leading edge at the column wall, and the resultant gradient induced band spreading.

### 3.5. *Effect of thermal conditions on efficiency*

In order to test the hypothesis presented in the preceding section, we conducted a series of experiments in which the thermal environment of the column would have a significant impact on the magnitude of any temperature gradients within the column. We did this by controlling the heat transfer across the column walls. As described in Section 2, we generated isopycnic plate height curves with the column in three different thermal environments within the column oven: water-thermostatted, air-thermostatted, and insulated. The analog system with column A was used, and temperatures at both the column inlet and outlet were monitored.

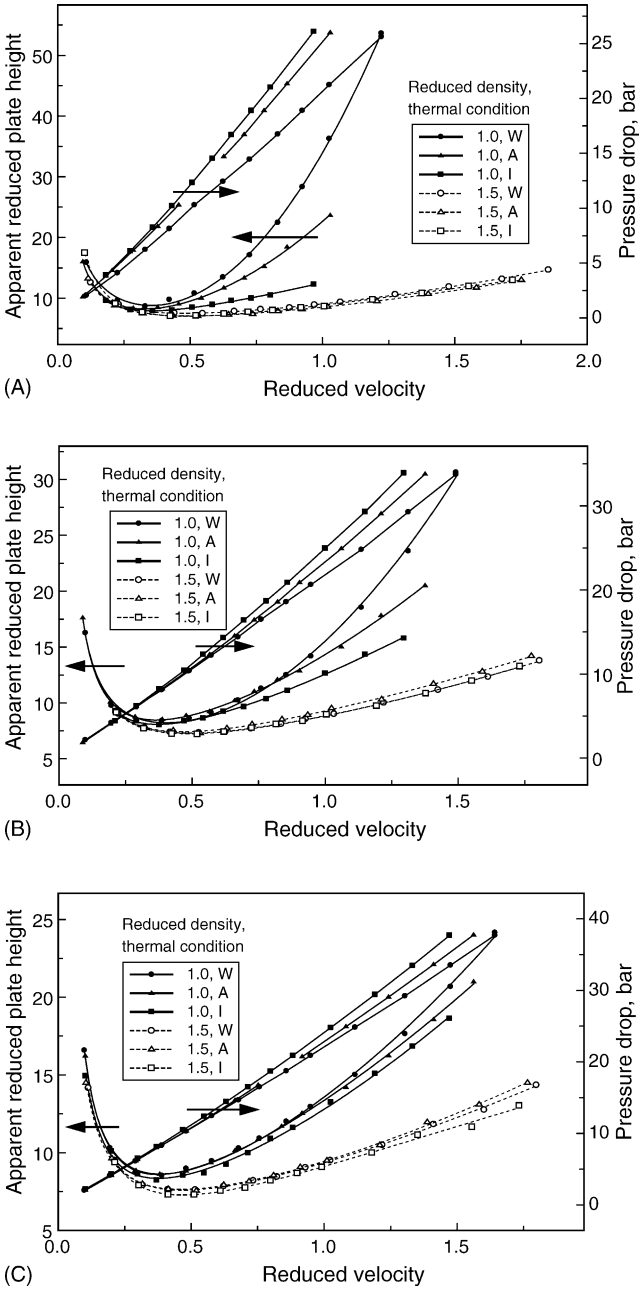


Fig. 9. Effect of thermal condition on efficiency for elution of methane using a water-thermostatted (W), air-thermostatted (A), and insulated column (I) at two reduced densities and oven temperatures of (A) 40.0 °C, (B) 50.0 °C, and (C) 60.0 °C, using column A and analog data collection. Water thermostatted at same temperature as column oven. See Fig. 5 for other conditions.

Plate height curves obtained under these three thermal environments were obtained at oven temperatures of 40, 50, and 60 °C and reduced densities of 1.0 and 1.5. The results are shown in Fig. 9. At the higher reduced density of 1.5 the efficiency is independent of the thermal environment and oven temperature, and is in all cases better than at the lower density. However, significant efficiency losses occur at the lower density, and the efficiency is dependent on the thermal environment, with the water-thermostatted column showing the

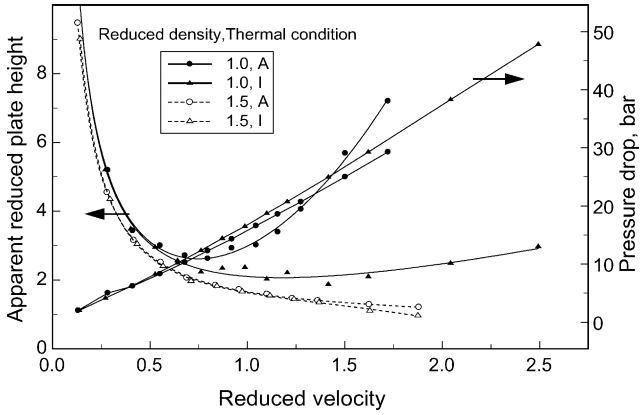


Fig. 10. Effect of thermal condition on efficiency for elution of methane at 50.0 °C using an air-thermostatted (A) and insulated column (I) with column B and digital data collection. See Fig. 6 for other conditions.

greatest losses. These effects are most apparent at the lower temperatures. The presence of thermal insulation provides the best efficiency at the lower density.

The experiments for the air-thermostatted and insulated cases were repeated using the digital system at an oven temperature of 50 °C and appear in Fig. 10. This system should provide a better measure of the true column efficiency under these conditions. The results confirm the trends observed with the slower analog system. A comparison of the low-density curves shows that most of the efficiency loss is eliminated by employing thermal insulation.

Column inlet and outlet temperatures for the studies conducted with the analog system appear in Fig. 11. At the lower density the temperature drops were quite large, especially for the air-thermostatted and insulated cases. Temperature drops of almost 8 °C were observed for the insulated column, and drops greater than 5 °C for the air-thermostatted column. Even for the water-thermostatted case temperature drops of

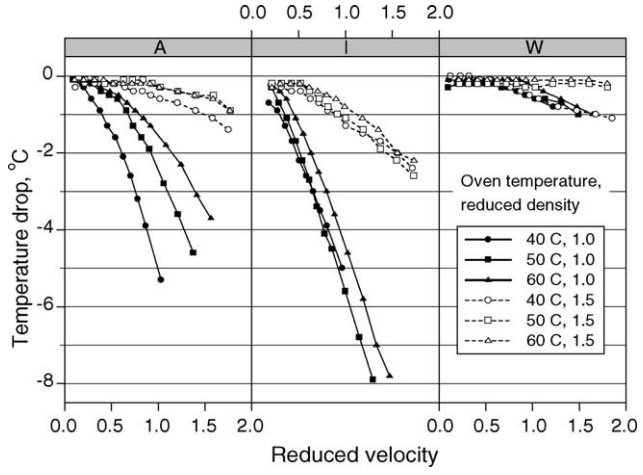


Fig. 11. Effect of thermal condition on temperature drop at three temperatures and two reduced densities. The thermal condition (A, I, W) is given in the top bar of each panel. See Fig. 9 for explanatory notes and operating conditions.

up to 1.0 °C were observed. At the higher density the temperature drops are smaller but still significant, reaching 2–3 °C for the insulated case, and about 1 °C for the air-thermostatted case. Even the water-thermostatted column at 40 °C showed a temperature drop of 1.1 °C at the highest velocity.

Of the three thermal modes employed, the insulated column shows the largest *axial* temperature gradients because the presence of thermal insulation effectively prevents heat flow across the column wall into the cooling fluid. As a result, there should be little or no *radial* temperature gradient produced in this case, and the efficiency curves in Figs. 9 and 10 show that at $\langle \rho_R \rangle_t = 1.0$ the insulated column shows the best efficiency. At the opposite extreme, the water-thermostatted column shows the smallest *axial* temperature gradients because heat is more effectively transported across the column wall into the cooling fluid, but this necessarily generates a large *radial* temperature gradient. The cooler fluid at the center of the column is more dense and more viscous than fluid near the walls, and its velocity is therefore lower than that of the warmer, less viscous fluid near the column wall, generating a parabolic band profile with the leading edge at the column wall as described earlier. As a result, gradient-induced band spreading is maximized for the water-thermostatted column. Air is not as good a heat transfer agent as water, and this case falls between the two extremes.

From these results we conclude that significant axial and radial temperature gradients are generated when packed columns are operated at large pressure drops under near-critical conditions, and that radial temperature gradients are responsible for much of the efficiency loss observed under these conditions. The radial temperature gradient can be suppressed by the use of thermal insulation, eliminating most of the efficiency loss.

Because this study has examined the efficiency of unretained solutes only, the interpretation of the results is not complicated by the effects of pressure and temperature gradients on retention factors. Two previous reports have examined the effects of thermal conditions on separations of retained solutes. Thermal insulation has been used to achieve significant improvements in both speed and efficiency [4] for elution of normal alkanes at 50 °C and $\langle \rho_R \rangle_t = 1.0$. The improved efficiency was attributed to the elimination of radial temperature gradients, while the decreased retention times were attributed to the axial temperature drop and the resulting increased mobile phase density. Bouigeon et al. [9] imposed a temperature gradient with a series of water jackets to maintain the column outlet at a lower temperature than the inlet. The lower outlet temperature decreased the magnitude of the density drop along the column, thereby minimizing changes in the retention factor, and significant improvements in efficiency were achieved. The present study on unretained solute indicates that the use of a water jacket can have a negative impact on efficiency due to the generation of radial temperature gradients. The use of thermal insulation on the column has the advantage of promoting an axial temperature gradient without the formation of significant radial temperature gradients.

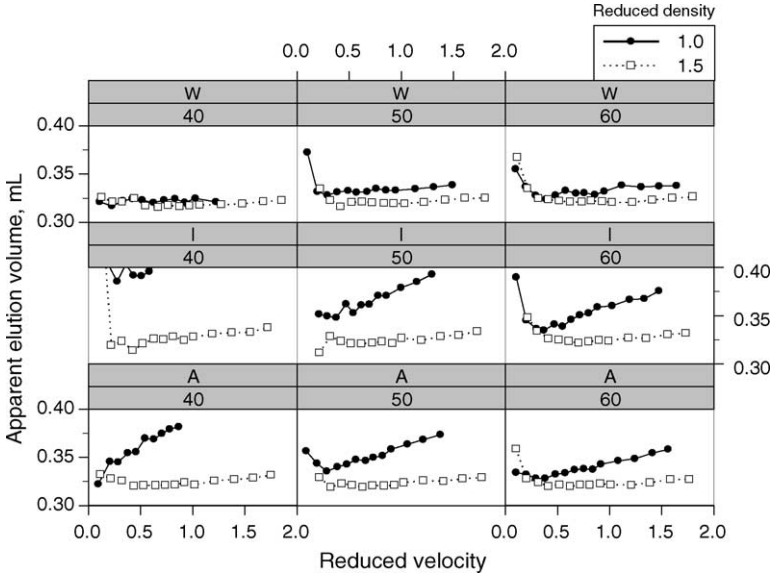


Fig. 12. Effect of temperature and thermal condition on apparent elution volume of methane. Bars above each panel give temperature in Celsius and thermal condition (A, I, W). See Fig. 9 for explanatory notes and operating conditions.

### 3.6. Pressure drop and reduced velocity

Because the pressure drop can have a direct impact on apparent plate height, we have included pressure drop data in the relevant figures. In general, the pressure drop required to achieve a given reduced velocity is roughly independent of the temperature or reduced density in Figs. 5 and 7, in accordance with the predicted behavior depicted in Fig. 4. The pressure drop required to achieve a given reduced velocity in Figs. 9 and 10, however, increases as one goes from water to air to insulation as the surrounding medium. The temperature data in Fig. 12 show that the magnitude of the temperature drop increases, or the average column temperature decreases, in the same order. A lower temperature results in higher mobile density and viscosity, requiring a larger pressure drop to achieve the same velocity. The pressure drop data are thus consistent with the observed temperature data. The foregoing argument is not rigorous, since Darcy's law predicts a linear relationship between pressure drop and velocity, not reduced velocity. We generated plots of pressure drop versus velocity (not shown) and found the same trends.

The column temperature drop does result in some errors in the reported values of reduced velocity. We have used reduced velocities in order to compensate for the effects of density on the diffusion coefficient and thus to directly compare plate height curves obtained at different mobile phase densities. Because we assumed isothermal conditions, the computed values of the diffusion coefficient, and therefore the reduced velocity, are not entirely accurate. For the case with the largest temperature drop we estimated the magnitude of the error in the reduced velocity due to this assumption to be approximately 11%. While not insignificant, the error is not so great as to affect the qualitative interpretation of the data.

### 3.7. Methane as an unretained solute

The predicted efficiency at $\langle\rho_R\rangle_t = 1.0$ represented in Fig. 6 assumes that methane is unretained. Elution of methane, ethane and propane under similar conditions on a Spherisorb C8 column does show some resolution of the three solutes [3], suggesting that methane may be slightly retained. For our interpretation of the data to be valid, it is important to demonstrate that methane is not significantly retained under our experimental conditions.

If there is any significant retention of methane, we would expect some increase in its elution volume with decreasing density. We therefore computed the *apparent* elution volumes for methane from the relation

$$V_R = \frac{t_R \dot{V}_p \rho_p}{\langle\rho_R\rangle_t \rho_c} \quad (6)$$

where $t_R$ is the retention time, $\dot{V}_p$ and $\rho_p$ are the volumetric flow rate at the pump and the density of the mobile phase at the pump, respectively, and $\rho_R$ and $\rho_c$ are the reduced density and critical density of carbon dioxide as defined earlier. This relation assumes that the mobile phase is at constant temperature and is at the target temporal average density, neither of which is strictly true. The apparent values of $V_R$ for the experiments on thermal conditions are shown in Fig. 12, plotted against reduced velocity to facilitate comparison to other figures in this paper. The apparent values of $V_R$ vary significantly, especially at $\langle\rho_R\rangle_t = 1.0$, but are roughly constant in the mid-range velocities at $\langle\rho_R\rangle_t = 1.5$. The combined effects of incomplete thermal equilibrium in the syringe pump and leakage of mobile phase past the pump seal are likely causes for deviations at the lowest velocities, where these effects have the greatest impact due to the low pumping rates and long elution times. At the higher velocities, a negative axial temperature

gradient would result in an average column density that is greater than assumed in Eq. (6), with the result that Eq. (6) predicts a value for $V_R$ that is too large. This is especially evident at $\langle\rho_R\rangle_t = 1.0$ for the insulated and air-thermostatted columns, where the temperature drop is greatest. Excluding the data at very low and high velocities, the apparent values of $V_R$ at $\langle\rho_R\rangle_t = 1.5$ are reasonably constant at 0.32 mL, regardless of the thermal environment, and we take this as the best measure of the elution volume for methane.

In order to determine the effect of density on $V_R$, we use the data for the water-thermostatted column, where the axial temperature drop is quite small. At 40 °C the values of $V_R$ are consistently about 0.32 mL at both densities, but at 50 and 60 °C, with a few exceptions, the values of $V_R$ at $\langle\rho_R\rangle_t = 1.0$ are consistently higher than at $\langle\rho_R\rangle_t = 1.5$ by a few percent. While this suggests some small degree of retention, the overall magnitude and changes in retention should be quite small and unlikely to have any significant impact on apparent plate height, and we conclude that methane is a suitable test solute for this investigation.

## 4. Conclusions

In this study we have examined the effects of pressure drop on efficiency for the unretained solute methane. This has allowed us to examine mobile phase effects without complications from variations in retention. Our major conclusions are:

(1) The efficiency loss when using large pressure drops under near-critical conditions is much greater than predicted by theory assuming isothermal conditions.
(2) Significant axial and radial temperature gradients are generated in packed columns with large pressure drops when using $CO_2$ mobile phase at average column pressures as high as 150 bar and temperatures up to 80 °C or more.
(3) For unretained solutes, radial temperature gradients are the major cause of efficiency loss under these conditions.
(4) At low densities and large pressure drops, the use of thermal insulation on the column can provide significant improvements in efficiency.

Though not addressed in this study, these conclusions are also relevant to retained solutes insofar as they are impacted by mobile phase effects. It is obvious, for example, that conditions affecting the rate of heat transfer across the column wall, such as air velocity or the wall material itself, can have a significant impact on retention and efficiency in pSFC at near-critical mobile phase densities and temperatures. Failure to carefully control these and other variables affecting heat transfer may help to explain why there has been some lack of agreement in the literature on the effects of pressure drop on efficiency.

Poppe et al. [7] have shown that the magnitude of the radial temperature gradient in HPLC is proportional to velocity, pressure drop and column radius. The same relationships should apply in SFC. This suggests that the use of smaller diameter columns should decrease the magnitude of the radial temperature gradient and result in improved efficiency. The effects of thermal conditions, particle size and column diameter for both retained and unretained solutes will be the subject of future communications on this topic.

## 5. Nomenclature

| | |
|---|---|
| $A$, $B$, $C$ | coefficients in the Knox equation for reduced plate height |
| $D_m$ | solute diffusion coefficient in the mobile phase |
| $d_p$ | particle diameter |
| $f_1$ | compressibility correction factor |
| $\hat{H}$ | apparent plate height |
| $h$, $\hat{h}$ | local reduced plate height, apparent reduced plate height |
| $t_r$ | retention time |
| $T$ | temperature |
| $V_R$, $\dot{V}_p$ | retention volume, volumetric flow rate of mobile phase at the pump |
| $w_h$ | peak width at half height |
| $L$ | length of column |
| $\nu$ | reduced velocity of mobile phase |
| $\rho$, $\rho_c$, $\rho_R$ | density of the mobile phase, critical density, reduced density ($\rho_R = \rho/\rho_c$) |
| $\rho_p$ | density of mobile phase at the pump |
| $\langle\rangle_t$, $\langle\rangle_z$ | for enclosed quantity: temporal average; spatial average |

## Acknowledgments

This work was supported by grants from the American Chemical Society Petroleum Research Fund (ACS PRF No. 31971-B9) and the University of Minnesota Graduate School Grant-In-Aid program.

## References

[1] D.P. Poe, J. Chromatogr. A 1078 (2005) 152.
[2] P.J. Schoenmakers, P.E. Rothfusz, F.C.C.J.G. Verhoeven, J. Chromatogr. 395 (1987) 91.
[3] D.P. Poe, P.J. Marquis, T. Tomlinson, J. Dohm, J. He, J. Chromatogr. A 785 (1997) 135.
[4] D.P. Poe, J. Chromatogr. A 785 (1997) 129.
[5] P.R. Sassiat, P. Mourier, M.H. Caude, R.H. Rosset, Anal. Chem. 59 (1987) 1164.
[6] H. Poppe, J.C. Kraak, J. Chromatogr. 282 (1983) 399.
[7] H. Poppe, J.C. Kraak, J.F.K. Huber, J.H.M. Van den Berg, Chromatographia 14 (1981) 515.
[8] D.P. Poe, J. Chromatogr. 625 (1992) 299.
[9] C. Bouigeon, D. Thiebaut, M. Caude, Anal. Chem. 68 (1996) 3622.